

Smart-Phone Energy Consumption Vs. 3G Signaling Load: The Influence of Application Traffic Patterns

Christian Schwartz, Frank Lehrieder, Florian Wamser, Tobias Hoßfeld, Phuoc Tran-Gia
University of Würzburg, Institute of Computer Science, Würzburg, Germany.

Abstract—The high signaling load in today’s UMTS networks has recently lead to severe problems and network outages of several hours, so called *Signaling Storms*. The reason is that certain network access patterns of popular smart-phone applications trigger frequent connection re-establishments, which are signaled to the network via the radio resource control (RRC) protocol. As a consequence of the network agnostic implementation of smart-phone applications, entities of the mobile network operator may experience overload, while energy consumption at the smart-phones is mutually determined.

The aim of this work is to study the impact of traffic characteristics on the power consumption of the smart-phone and the signaling messages in the mobile network. For that purpose, we first develop a simple model for the RRC states of a smart-phone. Second, we estimate the resulting power drain and the signalling traffic of the smart-phone. Then, we investigate the applicability of our model by comparing analytical with simulation results for real-world smart-phone traffic measurements. Finally, we evaluate the effect of network parameter optimization on traffic with different statistical characteristics. Our counter-intuitive results show that in particular bursty traffic patterns are suitable for UMTS networks while periodic patterns may cause increased power consumption and signaling overload – in contrast to classical queueing systems.

Index Terms—Signaling Storm, Energy Consumption, Smart-Phone Application, Radio Resource Control, 3G Networks

I. INTRODUCTION

The popularity of mobile broadband Internet access and the usage of smart-phone apps has grown tremendously during the last years. Apple reported that 10 billion apps have been downloaded from the *App Store*, while the Android market had around 150,000 apps available with about 350,000 downloads every day [1]. A success driver is the easy development of such an app compared to the early days of mobile phones. Today free or cheap development kits exist for each popular mobile platform which enable non-professionals or private users to create their own apps.

On the one hand, the easy development process of these smart-phone apps leads to huge number of diverse apps and enthusiastic popularity among end-users. On the other hand, this fosters a network-unaware implementation of the apps. As a result, the behavior of some apps does not take into account particular properties of mobile environments such as a limited battery capacity of the mobile phone, i.e. user equipment (UE) and utilization of wireless resources, e.g., the reservation of dedicated channels for long times. In today’s 3G UMTS networks, the allocation of dedicated and shared channels are controlled by the radio resource control (RRC) protocol [2].

This protocol defines a set of RRC states that the UE can take. The states have an important impact not only on the uplink and downlink transmission capacity that the UE can use, but also on the battery consumption of the UE. In addition, the RRC states depend on the demand to send or receive data. Therefore, the network access pattern of the used app has a crucial impact on the use of mobile network and battery resources.

In [3] increased control plane signaling is investigated due to frequent RRC state transitions. They identify excessive signaling overhead (both in RAN and in the CN) since occasional, very small update messages are sent. Especially, social networking applications on smart-phones are found to cause significant amount of signalling messages in 3G networks due to frequent status update messages on application layer. The authors highlight that traffic patterns from various applications yield to completely different signaling traffic in the mobile network. The 3GPP recently published a technical report [4] about use cases and potential network requirements to reduce the signaling overhead.

Our contribution is to investigate the trade-off between smart-phone energy consumption and the 3G signaling load. To estimate the impact of the network access pattern of a smart-phone on the consumption of wireless and battery resources, we develop a simple model for the RRC states of a UE in a 3G UMTS network. Our model assumes that the app sends and receives data packets according to a renewal process for a known distribution of the inter-packet time. From this information, we derive exactly the state distribution of the UE, i.e., the probability that the UE is in a specific state, and the frequency of state transitions. In addition, we model the consumption of wireless and energy resources for a given network access pattern. Based on real-world measurements of network traffic emerging from smart-phone apps, we compare analytical and simulative results to investigate the applicability of our model. As major contributions, we first provide a model for power consumption and signaling load emerging from smart-phone apps, and then identify characteristics of resource-efficient network access patterns.

The paper is structured as follows. Section II provides a background on 3G UMTS networks, the RRC protocol, and related work on measurements of relevant RRC parameters. The analytical model to quantify the trade-off between energy consumption and signaling load is derived in Section III. Numerical results and their implications are discussed in

Section IV. Section V concludes this work.

II. BACKGROUND ON UMTS AND THE RRC PROTOCOL

In general, a 3G UMTS mobile communication network consists of three components: user equipment (UE) like smart-phone or USB data stick, radio access network (RAN), and the core network (CN). The connection between UE and CN is established by the RAN. Within the RAN, the base station and the radio network controller (RNC) are responsible for radio resource control, packet scheduling, handover control, etc. The RNC is the controller for a set of base stations that are connected to it. The CN is the backbone network which forwards the user data to external networks such as the Internet or the public switched telephone network. It also provides support for other additional functions such as billing, authentication, or location management.

In UMTS networks, the radio resources in the RAN between base station and UE are controlled and managed with the help of the RRC protocol [2]. All the RRC procedures rely on protocol states which are defined to trigger certain protocol actions for different situations. If the UE is switched on and no connection to the mobile network is established, the UE is in *idle* state. In contrast, if the UE wants to send data, radio resources are allocated by the base station for the handset and the UE will go into *FACH* or *DCH* state. A corresponding channel for data transmission is assigned to the UE. The *FACH* and the *DCH* state can be distinguished in that way that in *DCH* state a high-power dedicated channel for high speed transmission is allocated whereas in *FACH* state a shared access channel for general sporadic data transmission is used. *FACH* significantly needs less power than *DCH*.

The possible transitions between the different states are defined by the network operator and the RRC protocol stack. Typically, the following state transitions are included: *idle* \rightarrow *FACH*, *FACH* \rightarrow *DCH* to switch from lower radio resource utilization and low UE energy consumption to another state using more resources and energy, and *DCH* \rightarrow *FACH*, *FACH* \rightarrow *idle*, *DCH* \rightarrow *idle* to switch to lower resource usage and energy consumption. According to [5], [6], the transitions are triggered by user activity and radio link control buffer level. A transition from *DCH* to *FACH* usually occurs when the buffer is empty and a threshold for a release timer is exceeded. The reverse direction is done if the buffer level oversteps a certain threshold value for a predefined time period. The UE goes into *idle* state if the RNC detects overload in the network or no data was sent by the UE for a certain time.

In literature, the configuration of the inactivity timers used of the RRC protocols have been investigated in detail. In [5] a measurement tool for RRC protocol states is presented. It is used to determine RRC state transition parameters, channel setup delays, and paging delay by measuring the one-way round trip time of data packets. The results are validated by monitoring the energy consumption in different RRC states. One outcome is that there are significant differences in UMTS network configurations. *DCH* release timer as well as the inactivity timer value to go into *idle* state were measured. The

values range from 1.2 s for *DCH* release timer to more than one minute for the *idle* timer. Similar results are presented in [6]. There, the values range from 5 s to 12 s. Additionally, they also determined the exact RRC state transitions for two networks such as *idle* \rightarrow *FACH* \rightarrow *DCH* or *idle* \rightarrow *DCH* directly without state *FACH*.

III. A SIMPLE PERFORMANCE MODEL FOR 3G RRC STATES

This section introduces the performance model for quantifying energy consumption against signaling load. After presenting the system description, we derive the state distribution and the average frequency of state transitions for a two-state model (*idle*, *DCH*), e.g. for proprietary fast dormancy implementations of smart-phone vendors [7]. Afterwards, we extend the model to include *FACH* for regular 3G networks. Finally, we define simple metrics for signaling load and energy consumption.

A. System Description and Basic Assumptions

We consider a smart-phone that sends and receives a sequence of data packets via a 3G UMTS network. The arrival process of the packet transmissions determines the RRC states of the smart-phone. However, the direction of packets (up-/downstream) has no impact on the RRC states, the states depend only on traffic activity. This is also the reason why we do not consider the packet size in our model. In real UMTS networks very small packets might be treated differently for RRC states, but we neglect this for simplicity reasons. Furthermore, the actual RRC state transitions are complex procedures depending on implementation details of the smart-phone, the used UMTS release, and the configurations by the network operator. In order to keep our model simply, but realistic, we reduce the set of standardized RRC states and the state transition triggers in the following ways.

In a first step we consider only a basic scenario with two RRC states: *idle* and *DCH* (cf. left part of Fig. 1). The UE switches to *DCH* to transmit or receive data and after an inactivity period of duration T_{DCH} it switches back to *idle*. The motivation for the two states RRC scenario is twofold. First, it serves for illustration purposes. We derive the model step-by-step in this simple scenario to explain the ideas behind

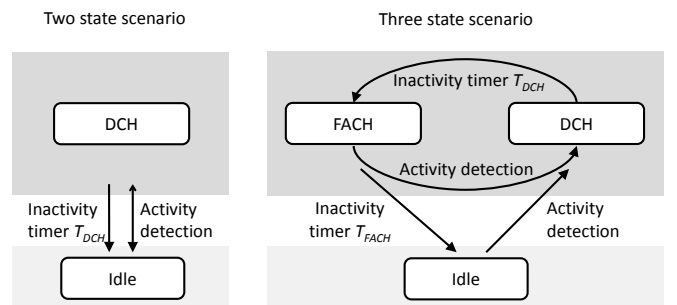


Fig. 1: Simplified RRC state transitions diagrams of the two state and the three state scenario.

the equations. The scenario is of practical relevance since proprietary implementations of the fast dormancy concept [7] exist, where UE decides to switch to idle shortly after the transmission of a packet without using any other RRC state. Furthermore, this model is very similar to the one found in Long Term Evolution (LTE) systems. In LTE, we only distinguish between connected and disconnected states.

In a second step we consider three RRC states (cf. right part of Fig. 1). The reason is that regular smart-phones are advised by the network to switch from state *DCH* to *FACH* after a certain inactivity period or when RRC buffers fall below certain thresholds. When the thresholds are exceeded, the UE is advised to switch back to *DCH* state. Otherwise, the UE switches to *idle* after an additional timeout T_{FACH} . However, we abstract from the RRC buffer thresholds in our model and consider only traffic activity since the thresholds in current networks are likely to be exceeded even for a single packet larger than 500 byte [8]. In addition, this permits to neglect the influence of the packet sizes in the model. A further motivation to include the *FACH* state is that the power drain of the UE is significantly smaller than in *DCH* state [6].

In our model we aggregate both packets sent and received by the UE in the packet arrival process, which is assumed to be a renewal process, i.e. a process with identical and independently distributed inter-arrival times, described by the random variable A (cf. Fig. 2). Thus, the probability that the time between two consecutive packets is at most t is $P(A \leq t) = A(t)$. We challenge this assumption by measurements of packet traces in Section IV-A.

B. The Case of Two RRC States

1) *State Distribution*: First, we are interested in the state distribution $P(S = s)$, i.e., the fraction of time that the UE spends in state $s \in \{idle, DCH\}$ for a given inter-packet time A . For this purpose, we define an observation interval T_{Obs} (cf. Fig. 2) that is orders of magnitude larger than the average inter-packet time $E[A]$. In addition, we take the position of an outside observer who observes the state s at a random point in time t^* , uniformly distributed within the observation interval. Then the state distribution $P(S = s)$ is the probability that the observer sees the UE in state s at t^* . We calculate this distribution according to

$$P(S = s) = \int_0^\infty q(\tau) \cdot P(S = s|A = \tau) d\tau, \quad (1)$$

where $q(\tau)$ is the probability density that t^* falls into an interval of length τ and $P(S = s|A = \tau)$ is the probability that the UE is in state s under the condition that t^* is within an interval of length τ .

We start with the derivation of $q(\tau)$. This probability density has to be proportional to $a(\tau)$ and to τ , where $a(\tau)$ is the probability density function of the random variable A . Therefore, we have that $q(\tau) = a(\tau) \cdot \tau \cdot c_0$ with the proportionality constant c_0 . Due to $\int_0^\infty q(\tau) d\tau = 1$, we have $c_0 = 1/E[A]$, which leads to

$$q(\tau) = \frac{a(\tau) \cdot \tau}{E[A]}. \quad (2)$$

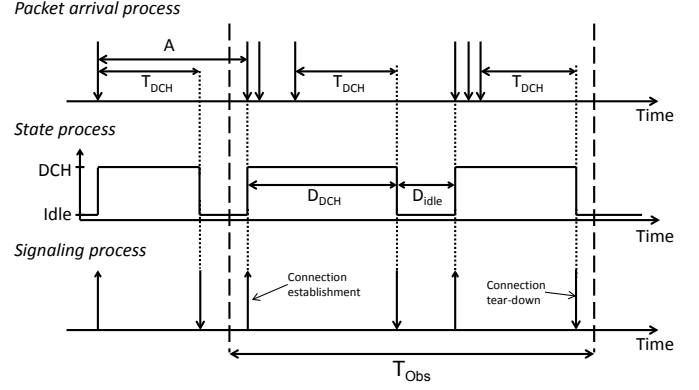


Fig. 2: Relation of packet arrival process (described by the random variable A), state process, and signaling process in the two state scenario.

Next, we derive the conditional probability $P(S = s|A = \tau)$ that t^* falls within a period with state s under the condition that the inter-packet time is $A = \tau$. We use the fact that t^* is uniformly distributed within τ and calculate the probability $P(S = idle)$ by case differentiation:

$$P(S = idle|A = \tau) = \begin{cases} 0, & \text{if } \tau \leq T_{DCH} \\ \frac{\tau - T_{DCH}}{\tau}, & \text{otherwise.} \end{cases} \quad (3)$$

The calculation for $S = DCH$ is very similar:

$$P(S = DCH|A = \tau) = \begin{cases} 1, & \text{if } \tau \leq T_{DCH} \\ \frac{T_{DCH}}{\tau}, & \text{otherwise.} \end{cases} \quad (4)$$

2) *Average Frequency of State Transitions*: Next, we estimate the average frequency of state transitions resulting from a given packet arrival process. For that purpose, we consider again the observation interval T_{Obs} and focus on the state transitions from *idle* to *DCH* since every switch from *DCH* to *idle* corresponds to a switch vice-versa. The expected number of observed packets during T_{Obs} is $E[n_p] = T_{Obs}/E[A]$. Furthermore, the probability that time between two consecutive packets exceeds the timer T_{DCH} is

$$P(A > T_{DCH}) = 1 - P(A \leq T_{DCH}) = 1 - A(T_{DCH}). \quad (5)$$

The number of state transitions $n_{idle \rightarrow DCH}$ during T_{Obs} directly corresponds to the number of inter-packet times exceeding T_{DCH} since an active connection is torn down after an inactivity period of T_{DCH} . Therefore, the expected number is

$$\begin{aligned} E[n_{idle \rightarrow DCH}] &= E[n_p] \cdot P(A > T_{DCH}) \\ &= \frac{T_{Obs}}{E[A]} \cdot (1 - A(T_{DCH})). \end{aligned} \quad (6)$$

Hence, the expected frequency of state transitions is

$$E[f_{idle \rightarrow DCH}] = \frac{1 - A(T_{DCH})}{E[A]}. \quad (7)$$

The same holds also for the state transitions from *DCH* to *idle* and hence $E[f_{DCH \rightarrow idle}] = E[f_{idle \rightarrow DCH}]$.

C. Extension for Three RRC States

In this section, we consider three states: *idle*, *DCH*, and *FACH*. We assume that the UE switches from *idle* to *DCH* whenever it transmits or receives data. After an inactivity of T_{DCH} the UE switches to *FACH*, and after an additional inactivity of T_{FACH} , it switches to *idle* (cf. right part of Fig. 1).

1) *State Distribution*: The state distribution $P(S = s)$ for the three states $s \in \{idle, FACH, DCH\}$ can be derived in the same way as for the scenario with two states. Therefore, we present only the conditional probabilities (which differ from the two state case) and use Eq. (1) for the calculation of the distribution. We start with $S = idle$:

$$P(S = idle|A = \tau) = \begin{cases} 0, & \text{if } \tau \leq T_{DCH} + T_{FACH} \\ \frac{\tau - (T_{DCH} + T_{FACH})}{\tau}, & \text{otherwise.} \end{cases} \quad (8)$$

For the case of $S = FACH$, we have:

$$P(S = FACH|A = \tau) = \begin{cases} 0, & \text{if } \tau \leq T_{DCH} \\ \frac{\tau - T_{DCH}}{\tau}, & \text{if } T_{DCH} < \tau \leq T_{DCH} + T_{FACH} \\ \frac{T_{FACH}}{\tau} & \text{if } \tau > T_{DCH} + T_{FACH} \end{cases} \quad (9)$$

The probability for the *DCH* state $P(S = DCH|A = \tau)$ does not differ from the two state scenario (cf. Eq. (4)).

2) *Average Frequency of State Transitions*: In contrast to the two state scenario, we have to consider a larger number of state transitions. These are the transitions from *idle* to *DCH*, from *DCH* to *FACH*, from *FACH* to *DCH*, and from *FACH* to *idle*. Other transitions do not occur. We first calculate the frequency of state transitions from *DCH* to *FACH*. This transition happens every time when the inter-packet time A exceeds the timer T_{DCH} . Therefore, the derivation is the same as presented above:

$$E[f_{DCH \rightarrow FACH}] = \frac{1 - A(T_{DCH})}{E[A]}. \quad (10)$$

$$E[f_{FACH \rightarrow idle}] = \frac{1 - A(T_{DCH} + T_{FACH})}{E[A]}. \quad (11)$$

Furthermore, all state transitions from *FACH* to *idle* correspond to a switch from *idle* to *DCH* and therefore $E[f_{idle \rightarrow DCH}] = E[f_{FACH \rightarrow idle}]$. Finally, we calculate $E[f_{FACH \rightarrow DCH}]$. This happens when $T_{DCH} < A \leq T_{DCH} + T_{FACH}$. Therefore, we have

$$E[f_{FACH \rightarrow DCH}] = \frac{A(T_{DCH} + T_{FACH}) - A(T_{DCH})}{E[A]}. \quad (12)$$

Other state transitions do not occur in our scenario (cf. Fig. 1).

D. Modeling Signaling Intensity and Power Drain of the UE

We assume that every state transition involves signaling traffic. In order to quantify signaling load on an abstract level, we define the *signaling intensity* SI of an application (i.e., of a given distribution for A) as the average number of state transitions required for the transmission of a single data packet.

$$SI = \frac{E[f_{ST}] \cdot T_{Obs}}{E[n_P]} = E[f_{ST}] \cdot E[A] \quad (13)$$

where $E[f_{ST}]$ is the sum of all state transitions. Consequently, $SI \in]0, 2]$ for the two state scenario since every packet can at most cause two state transitions (in the three state scenario it is $SI \in]0, 3]$). This metric is intended to quantify the relation between transmitted data packets and the involved RRC state transitions, which all incur mobile network signaling. The metric can be extended to capture more details, such as the number and type of signaling messages exchanged for a specific state transition. Since we use this metric for more qualitative analysis of source traffic produced by smart-phone applications, we stick to the definition above allowing for an illustrative understanding of the numerical results.

Next, we model the *battery drain of the UE* due to the UMTS transmission unit. We assume three power levels PD_s , one for every state s and calculate the average power drain PD based on the state distribution, which in turn depends on the packet arrival process A .

$$PD = \sum PD_s \cdot P(S = s) \quad (14)$$

with $s \in \{idle, DCH\}$ or $s \in \{idle, FACH, DCH\}$ depending on the scenario. This is a user-centric metric and gives insights into how efficient the transmission process uses the battery.

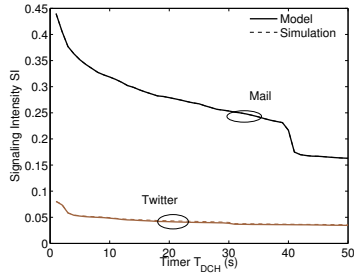
IV. NUMERICAL EXAMPLES AND THEIR IMPLICATIONS

First, we validate our performance model by comparing the analytical results with simulations based on measured packet traces of two real smart-phone applications. Then, we investigate the impact of traffic patterns on signaling load and power drain and derive high-level implications of the model.

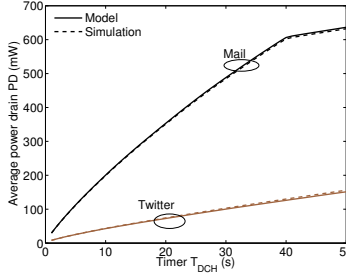
A. Model Validations

In order to assess the applicability of our performance model, we first have to check whether real-world application traces can be modeled as renewal process, which was our main assumption for the model. We use the Lewis-Robinson-Test [9], which is a hypothesis test with null hypothesis H_0 that the tested process is a renewal process. To this end, we use exemplary the measurement results for two different types of applications: Twitter and Mail. According to this test, the null hypothesis cannot be rejected for both of our packet traces at a significance level of 95%. Although this assumption may not be true for all applications, our results show that at least the considered applications can be modeled as a renewal process. More details on the measurement setup can be found in [10].

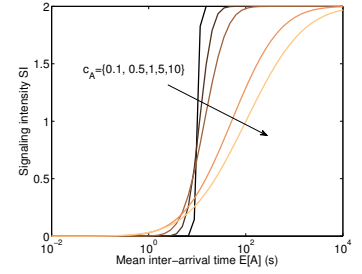
Next, we compare our analytical performance results with RRC protocol simulations using measured application and TCP traces which are described in detail in [10]. In order to produce analytical results that correspond to the real applications, we extract the empirical distributions of the inter-packet time A from the traces for both applications and use these distributions as input for Eq. (2). In Fig. 3a and Fig. 3b we compare the accuracy of the results obtained by the presented method to the values obtained from simulations for the two measured applications. We observe that the accuracy for both power drain (PD) and signaling intensity (SI) is very high. In Fig. 3a the results for the Mail application obtained by the model completely align with those obtained by the simulation.



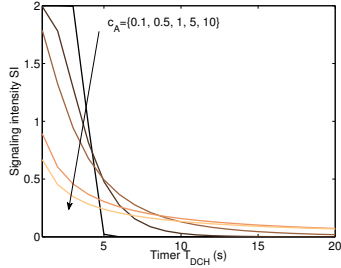
(a) Performance model vs. simulations wrt. signaling intensity in the three state scenario.



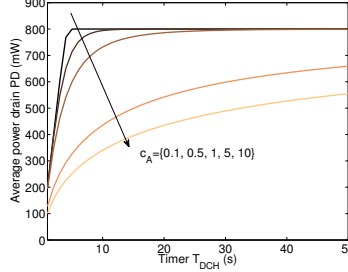
(b) Performance model vs. simulations wrt. power drain in the three state scenario.



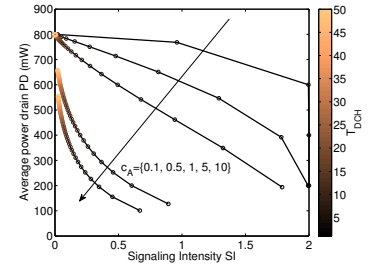
(c) Signaling intensity (two state, with $T_{DCH} = 10$ s) for different traffic patterns.



(d) Signaling intensity SI (2-State) or different timeout values T_{DCH} and coefficient of variations c_A .



(e) Average power drain PD (with $T_{DCH} = 10$ s) for different timeout values T_{DCH} and coefficient of variations c_A .



(f) Average power drain PD and signaling intensity SI for different timeout values T_{DCH} and coefficients of variations c_A .

Fig. 3: Validation of the performance model with 3G simulations (a),(b). Numerical results for signaling intensity (c),(d) and power drain (e) depending on application traffic pattern. Trade-off between power drain against signaling load (f).

B. Impact of Traffic Patterns on Signaling Intensity

First, we focus on the signaling intensity SI of traffic patterns and check the impact of the average inter-packet time $E[A]$ and the timer configuration. The signaling intensity SI , i.e., the average number of state transitions required for the transmission of a single packet, is an abstract measure for the signaling load produced by a specific traffic pattern.

1) *Impact of the Average Inter-Packet Time $E[A]$* : Some applications, for example those downloading or streaming of videos, send and receive large amounts of data within short time frames. In contrast, other applications such as social network clients send and receive small amounts of data every few minutes over the time span of some hours or days. In this section we study the impact of average inter-packet times $E[A]$ and the burstiness of the traffic pattern, i.e., the coefficient of variation $c_A = \sqrt{\text{Var}[A]}/E[A]$ on the signaling load. For that purpose, we use the simple two state scenario, set the timer $T_{DCH} = 10$ s, consider only the first and the second moment of the inter-packet time A , and assume that A follows a lognormal distribution, where both moments can be varied independently.

In Fig. 3c, we vary the average inter-packet time $E[A]$ in six orders of magnitude and investigate the resulting signaling intensity SI for different coefficients of variation c_A . We observe that c_A has no impact on SI for very small inter-packet times $E[A] < 10^{-1}$ s. The reason is that the UE stays in state DCH for all the time since no inter-packet times $A > T_{DCH}$ occur. In addition, the impact of c_A is small for very large values of $E[A] > 10^3$. There, the UE switches to

state DCH and back to state $idle$ for the transmission of every packet. Therefore, the signaling intensity SI approaches the value 2. For values in between these two extremes, the coefficient of variation c_A has a considerable impact on the signaling intensity SI . More periodic traffic (small values of c_A) make the increase of SI from 0 to 2 very sharp at the value $E[A] = T_{DCH}$, while this increase is more smooth for larger values of c_A . This is because for nearly periodic traffic it is crucial whether the timer value T_{DCH} is smaller or larger than $E[A]$. For larger values of c_A this dependency is weaker.

Next, we focus on the impact of the timer value T_{DCH} with respect to the burstiness of the traffic. We use the same setting as before, but fix the average inter-packet time $E[A] = 4$ s. While there are differences in $E[A]$ among users in real world settings, measurement studies have revealed that across all users 95% of the packets are received or transmitted within 4.5 seconds of the previous packet [11]. Therefore, the order of magnitude of $E[A] = 4$ s is of practical relevance. The signaling intensity SI is shown in Fig. 3d with respect to the timer value T_{DCH} and the burstiness c_A of the traffic pattern. Obviously, larger timers lead to less frequent state transitions and therefore to less signaling load. We observe in addition that the impact of the timer is crucial for nearly periodic traffic. If the average inter-packet time for nearly periodic traffic is larger than the timer, then every packet transmission involves a state transitions from $idle$ to DCH and a transition back. In contrast, no transitions are required if the average inter-packet time is longer than the timer. With increasing values

of c_A the impact of the timer is reduced. This means that for bursty traffic patterns the timer value is of less importance with respect to the generated signaling load.

C. Impact of Traffic Patterns on Power Drain PD of the UE

In this section we study the impact of the traffic patterns on the power drain PD of the UE. This metric quantifies how resource-efficient specific traffic patterns and timer configurations are for the battery of the UE. For the power drain in the different RRC states, we use the radio network power measured in a commercial UMTS network [6]: $PD_{DCH} = 800$ mW, $PD_{FACH} = 460$ mW, and $PD_{idle} = 0$ mW. We investigate the impact of the average inter-packet time, the impact of the timer configuration and validate our model with simulations. In Section IV-B1 we have seen that no state transitions occur for very small and very large average inter-packet times $E[A]$. Thus, traffic patterns with very small and very large inter-packet times $E[A]$ have also no impact on the power drain of the UE regardless of the burstyness represented by the coefficient of variation c_A .

To study the impact of the timer configuration T_{DCH} , we use the same setting as for the signaling load: lognormal distribution of inter-packet time A , $E[A] = 4$ s, two state scenario. The numerical values (c.f. Fig. 3e) show that longer timeouts lead to a higher power drain PD . This is reasonable since the UE stays longer in the power intensive DCH state in these cases. However, we observe that the burstiness of the traffic pattern has also a considerable impact on the power drain PD . The reason is that bursty traffic patterns send a lot of traffic during short periods when the UE is in state DCH anyway. During the following off-periods that UE can save energy in $idle$ state. Hence, we conclude that longer timeouts and smaller coefficients of variation c_A (more periodic and less bursty traffic) lead to a higher power drain of the UE.

D. Trade-off: Energy Consumption vs. Signaling Load

In Fig. 3f, we show the effect of network parameter optimization using the timer T_{DCH} on traffic patterns with varying coefficient of variation. We see that optimizations may decrease signaling by large amounts while only having very little impact on power consumption for one specific kind of traffic. The same timer setting could increase the power consumption for another kind of traffic while only offering little benefit with regard to the generated signaling intensity.

In [10] we discuss this effect in more detail suggest alternatives to network parameter optimization. One such alternative would be the use of Network Function Virtualization. Here, network entities are realized in software and deployed in the cloud, allowing for dynamic scaling. However, while this alleviates some of the symptoms it does not solve the general problem of network unaware applications or reduce the UE power consumption. To remedy this problem in the long term, the Future Internet should allow applications to incorporate information about the network state in the application logic, enabling cooperation between app and network. One such approach is Economic Traffic Management [12]. Here, the

stakeholders cooperate by exchanging information in order to reach a joint optimization goal. This concept could be applied by ensuring that the hardware vendor provides interfaces to the application developer allowing traffic to be sent at times when power use and incurred signaling cost would be minimal.

V. CONCLUSION

In this work we developed a simple model in order to estimate the signaling load and power drain of smart-phone applications with respect to their network access patterns. We tested the applicability of our model with simulations based on packet traces of two popular smart-phone applications. Our results show that different access patterns have a considerable impact on the required resources of the mobile phone and the network. We identified bursty traffic pattern as particularly resource-efficient with respect to energy consumption and signaling load. In contrast, nearly periodic traffic is likely to cause signaling overload due to frequent connection re-establishments, especially when the connection timeout is slightly below the inter-packet time. Optimization of network parameters may on one hand decrease the signaling occurring in the network, but can on the other hand increase the power consumption to unacceptable levels for the end-users.

REFERENCES

- [1] M. Butler, "Android: Changing the mobile landscape," *IEEE Pervasive Computing*, vol. 10, no. 1, pp. 4–7, 2011.
- [2] *TS 25.331, Radio Resource Control (RRC); Protocol specification*, 3GPP Std., 2012. [Online]. Available: <http://www.3gpp.org/ftp/Specs/html-info/25331.htm>
- [3] Signals Research Group, LCC, "White paper: Smartphones and a 3G network, reducing the impact of smartphone-generated signaling traffic while increasing the battery life of the phone through the use of network optimization techniques," 2010.
- [4] *TR 22.801, Study on non-MTC Mobile Data Applications impacts (Release 11)*, 3GPP Std., 2011. [Online]. Available: <http://www.3gpp.org/ftp/Specs/html-info/22801.htm>
- [5] P. Perala, A. Barbuizi, G. Boggia, and K. Pentikousis, "Theory and practice of RRC state transitions in UMTS networks," in *Proceedings of the global communication conference (GLOBECOM) Workshops*, 2009.
- [6] F. Qian, Z. Wang, A. Gerber, Z. Mao, S. Sen, and O. Spatscheck, "Characterizing radio resource allocation for 3G networks," in *Proceedings of the 10th annual conference on Internet measurement (IMC)*, 2010.
- [7] NokiaSiemensNetworks, "White paper: Understanding smartphone behavior in the network," 2011.
- [8] F. Qian, Z. Wang, A. Gerber, Z. Mao, S. Sen, and O. Spatscheck, "Profiling resource usage for mobile applications: a cross-layer approach," in *Proceedings of the 9th international conference on mobile systems, applications, and services (MobiSys)*, 2011.
- [9] H. Ascher and H. Feingold, *Repairable Systems Reliability: Modeling, Inference, Misconceptions and Their Causes*. Marcel Dekker, Inc., 1984.
- [10] C. Schwartz, T. Hoßfeld, F. Lehrieder, and P. Tran-Gia, "Angry Apps: The Impact of Network Timer Selection on Power Consumption, Signalling Load, and Web QoE," *Journal of Computer Networks and Communications*, 2013.
- [11] H. Falaki, D. Lymberopoulos, R. Mahajan, S. Kandula, and D. Estrin, "A first look at traffic on smartphones," in *Proceedings of the 10th annual conference on Internet measurement (IMC)*, 2010.
- [12] T. Hoßfeld, D. Hausheer, F. Hecht, F. Lehrieder, S. Oechsner, I. Papafili, P. Racz, S. Soursos, D. Staehle, G. D. Stamoulis, P. Tran-Gia, and B. Stiller, "An Economic Traffic Management Approach to Enable the TripleWin for Users, ISPs, and Overlay Providers," in *FIA Prague Book*, G. Tselentis *et al.*, Eds. Towards the Future Internet – A European Research Perspective: IOS Press Books Online, May 2009, pp. 24 – 34.